Mauna Loa Weekly CO2 Data

Data Analysis:

Figure 1 shows the atmospheric CO_2 concentration measured weekly at the Mauna Loa Observatory (see Ref.1) for the period 29 March 1958 to 29 November 2025. The Observatory is at Latitude 19.54° North, Longitude 155.57° West, Elevation 3397 metres. It is on the northern slope of Mauna Loa, an active volcano on the island of Hawai'i in the mid-North Pacific Ocean.

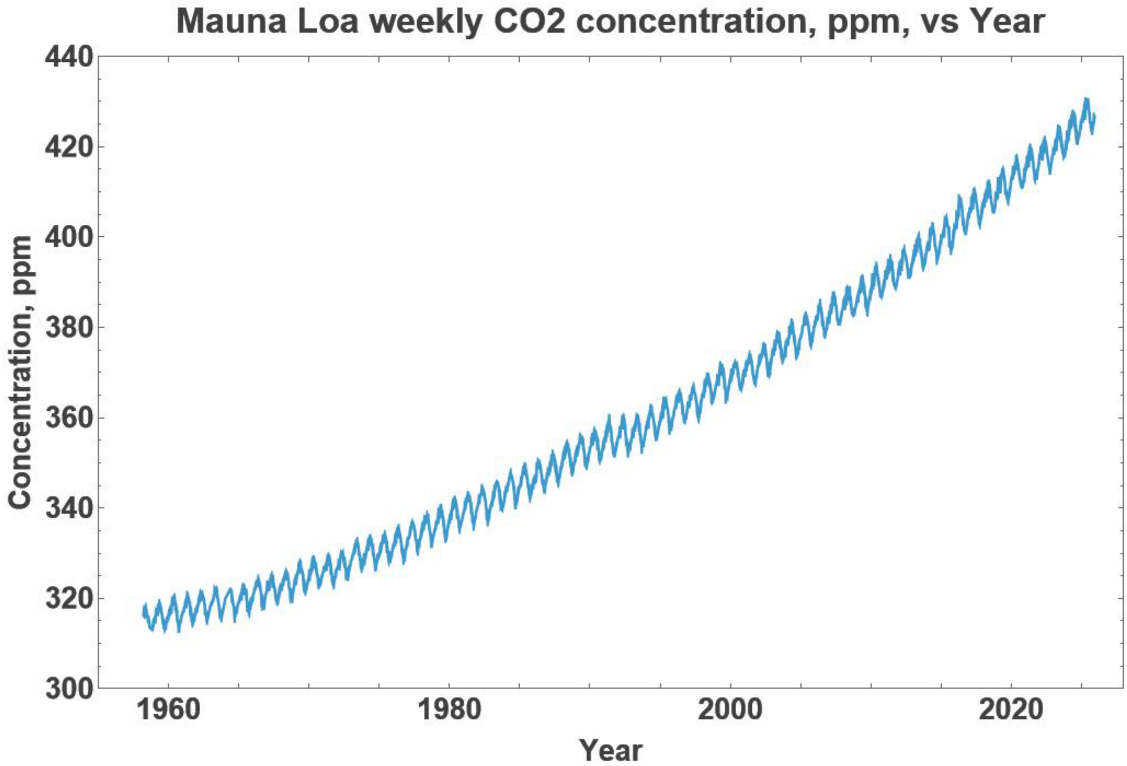

Figure 1. Mauna Loa weekly CO_2 concentration

As there were missing values in the time sequence, interpolation was applied using a fourth order polynomial fit to adjoining data strings and a weekly time interval of 7.0 days, for the following analysis of the CO_2 concentration time series. The original time series consisted of 3457 values while the interpolated time series consisted of 3532 values at a uniform weekly interval.

The series shows a regular seasonal variation superimposed on an upward trend. The linear trend for the whole period of 67 years was 1.65 ppm per annum. For the 5 year period 29 March, 1958 to 23 March 1963, the rate was 0.72 ppm pa. For the 5 year period 05 December 2020 to 29 November 2025, the rate had steadily increased to 2.62 ppm pa, that is 3.66 times greater than 62 years earlier. The acceleration in the rate of generation of CO_2 over the time of the measurements is attributed to an increase in the source of CO_2 relative to the sinks in response to the gradual increase in temperature since the end of the Little Ice Age. Justification for this claim is that the increase in the Sun's temperature has been greatest in the Equatorial zone and minor at the Poles. As the solubility of CO_2 decreases with increasing temperature more CO_2 effervesces from the large area of Equatorial ocean with little change in the absorption of CO_2 over the small area of the Poles. In the Equatorial zone the Sun is vertically overhead twice per year while in the Polar regions the Sun is at a shallow angle to the surface for half of a year and absent for the other half.

There are three inflections in the graph corresponding to the time of the volcanic eruptions at Mount Agung, Bali, Indonesia, 17 March and 16 May, 1963, Mount Pinatubo, Philippines, 12 June 1991, and Kilaueu, Hawai`i, May 2018. A step in the CO_2 concentration appears to have occurred due to each volcanic eruption. The Mauna Loa Observatory is 9598 km on a bearing of 71°East from Mount Agung, 8859 km on a bearing of 72°East from Mount Pinatubo and 4226 km on a bearing of 82°West from Kilaueu. These events contrast with the lack of any change in the accelerating rate of increase of CO_2 during the reduction of economic activity from the 2019 pandemic or the current 'Net Zero' effort negating the claim that CO_2 has been increasing due to the human activities.

The amplitude of the seasonal variation ranged from 5.72 ppm, 17 October 1970 to 15 May 1971, to 10.10 ppm, 12 September 2015 to 09 April 2016, changing from year to year in an irregular fashion but clearly increasing in amplitude over time. The maximum in the seasonal variation occurred during the early Summer months. As the seasonal variation in temperature and climate are driven by the change in the Sun's irradiation as the Earth orbits the Sun annually, it is the seasonal temperature/climate change that causes the change in CO_2 concentration not the reverse. CO_2 concentration change does not cause the temperature or climate of the Earth to change as claimed by the UN IPCC.

The annual rate of change of the CO_2 concentration was determined from the interpolated weekly time series by taking the difference between values 52.8211 weeks apart, being the average number of weeks in a year, and is shown in Figure 2. It displays the estimated annual rate of change of CO_2 concentration with high frequency noise superimposed on a cyclic pattern with a positive linear trend of 0.029 ppm pa per annum.

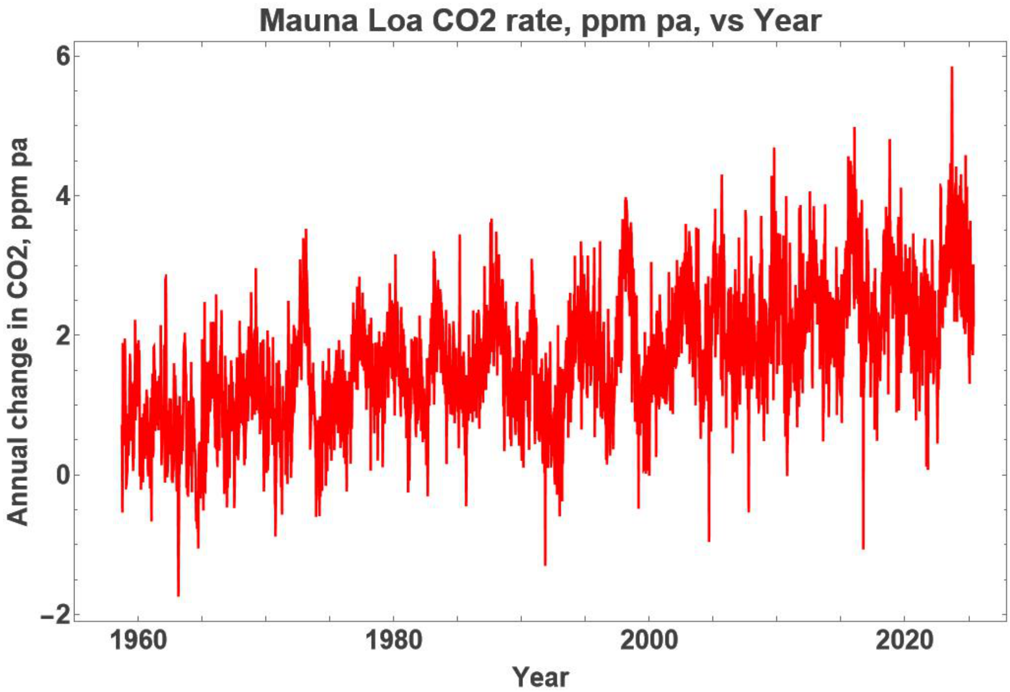

Figure 2. Mauna Loa annual rate of change of CO_2 concentration.

The least annual rate of change of -1.68 ppm pa per annum occurred in the 12 month period centred at 23 February 1963, possibly due to the major volcanic eruption of Mount Agung, Bali, Indonesia, 17 March and 16 May, 1963, and the greatest rate of change was 5.79 ppm pa per annum in the 12 month period centred at 09 September 2023. The linear rate of increase in Figure 2 is 0.029 ppm pa throughout the 67 years of recording regardless of the efforts of mankind to reduce the atmospheric CO2 concentration.

The sequence of maxima and minima for the annual rate of change of CO2 concentration matches that for the Oceanic Niño 3.4 Index (Ref.2). In order to better illustrate the correlation between the two series, Figure 3 shows the detrended Mauna Loa annual rate of change of CO_2 concentration, after smoothing with a low pass filter, overlain on the Oceanic Niño 3.4 Index, both covering the same 68 year period. In considering the relationship between the two series it is necessary to be aware that the Mauna Loa rate of change was derived from a weekly series of measurements taken at a single point on the globe. The Oceanic Niño 3.4 Index is the anomaly in the sea surface temperature relative to a 30 year average over the Equatorial zone between latitudes 5° South to 5° North and longitudes 120° West to 170° West, an area of the central Pacific Ocean of 6,568,670 square kilometres. The Mauna Loa Observatory is 2,450 km from the centre of the Ninõ 3.4 area, on a bearing of 27.5° East of North.

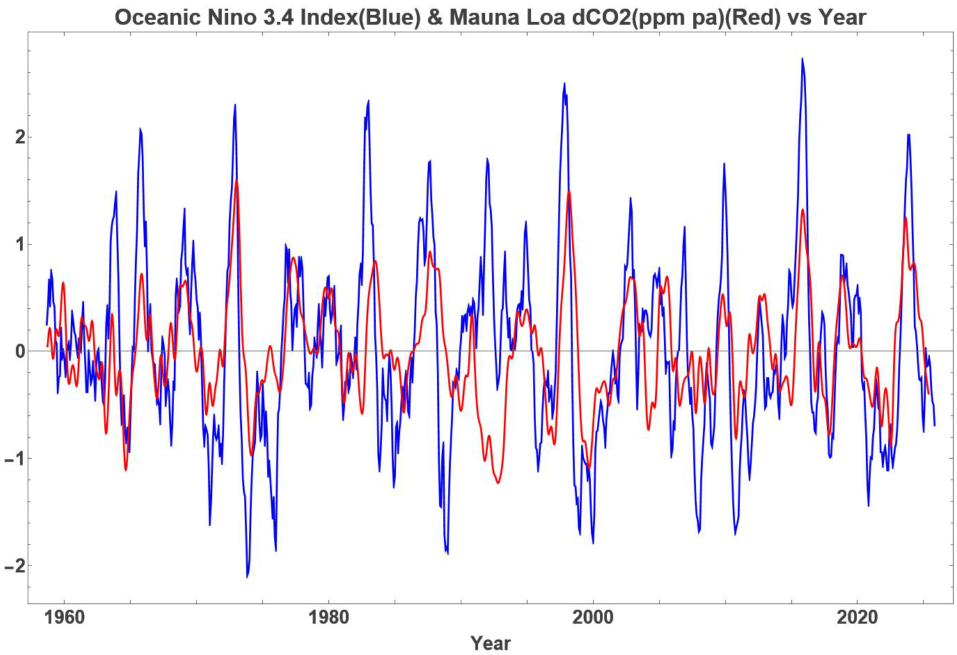

Figure 3. Overlay of the Oceanic Niño 3.4 Index and the Mauna Loa smoothed, detrended CO_2 annual rate of change.

As has been demonstrated in earlier studies of CO_2 data on the Climate Auditor web pages, their seasonal variation has been attributed to the associated temperature change. Likewise the close correlation between the Mauna Loa CO_2 rate of change and the Oceanic Niño 3.4 Index, as shown by the coincidence of the major maxima in Figure 3, is attributed to the decrease in the solubility of CO_2 to the maxima in sea surface temperature bought about by the major, world-wide climate event depicted by the Niño 3.4 Index.

There is a marked negative correlation in the centre of the graph in the later part of 1991 following the major volcanic eruption of Mount Pinatubo in the Philippines on 12 June 1991 which significantly altered the relationship between the rate of change of CO_2 and the Oceanic Niño 3.4 Index. The eruption caused the rate of change of CO_2 to drop to a minimum as the seasurface temperatures reached a local maximum. The eruption may not have been reflected in the ONI 3.4 seasurface temperatures as Mount Pinatubo is 1675 km North of the Equator well outside the ONI 3.4 area.

Autocorrelation Function:

More detail of the source of variation in the CO_2 annual rate of change is shown by its autocorrelation function illustrated in Figure 4. It reveals a clear cyclic pattern based on the El Niño event as shown in the accompanying table listing the correlation maxima, Table 1.

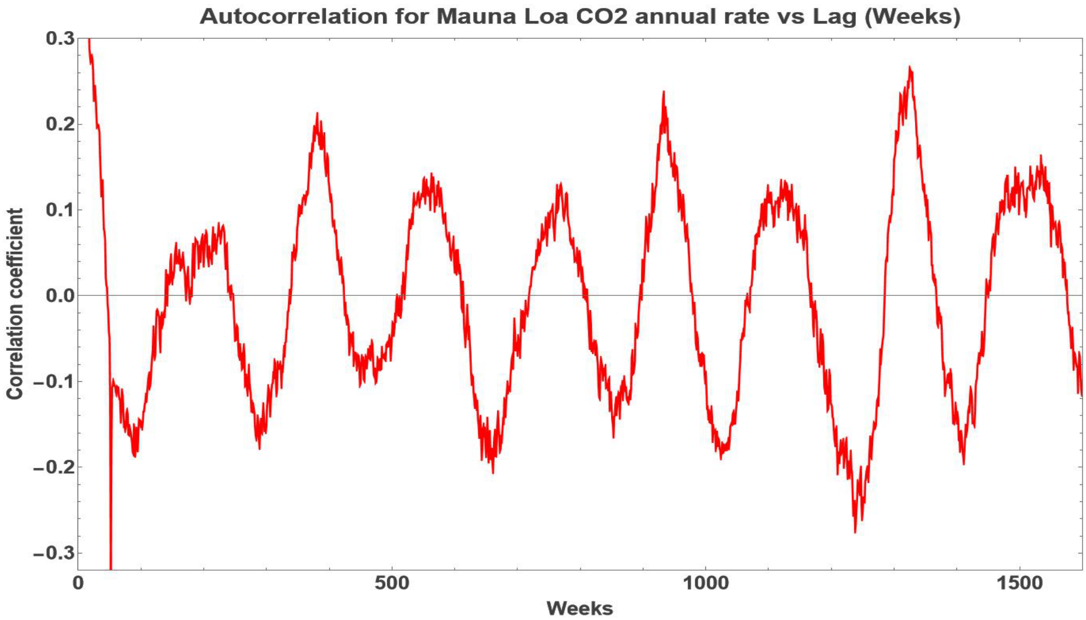

Figure 4. Autocorrelation for CO_2 annual rate of change.

Table 1. Autocorrelation maxima

Amplitude	Years	Weeks	Days	Source
0.059	2.99	156.0	1092	pre-El Niño
0.081	4.43	231.0	1617	post-El Niño
0.211	7.30	381.0	2667	2 x El Niño
0.140	10.79	563.0	3941	3 x El Niño
0.130	14.74	769.0	5383	4 x El Niño
0.236	17.88	933.0	6531	5 x El Niño
0.133	21.46	1120.0	7840	6 x El Niño
0.265	25.39	1325.0	9275	7 x El Niño
0.161	29.40	1534.0	10738	8 x El Niño

The average from Table 1, column 4, adjusted for the multiple expressions of the El Niño event was 1328 days. The event clearly dominates the CO_2 annual rate of change indicating that this major climate event determines the rate of generation of CO_2 in the Equatorial region confirming the earlier proposition that the temperature level determines the rate of change of CO_2 concentration as seen in the monthly data for Cape Grim and Macquarie Island stations and Mt Waliguan Observatory described in the analysis of data from each site and reported in the pages of: https://www.climateauditor.com .

Discrete Fourier Transform:

Figure 5 shows the amplitude spectrum from the Discrete Fourier Transform of the interpolated time series for the detrended annual rate of change of the CO2 concentration series length of 3479 values. The amplitude scale was clipped to better display the higher frequency, shorter wavelength events so it excludes the maximum of 8.48 at x-coordinate 18, equivalent to a period of 1353 days, which dominated the autocorrelation function. This confirms the maximum predicted to represent the response to the El Niño event already seen in the autocorrelation function.

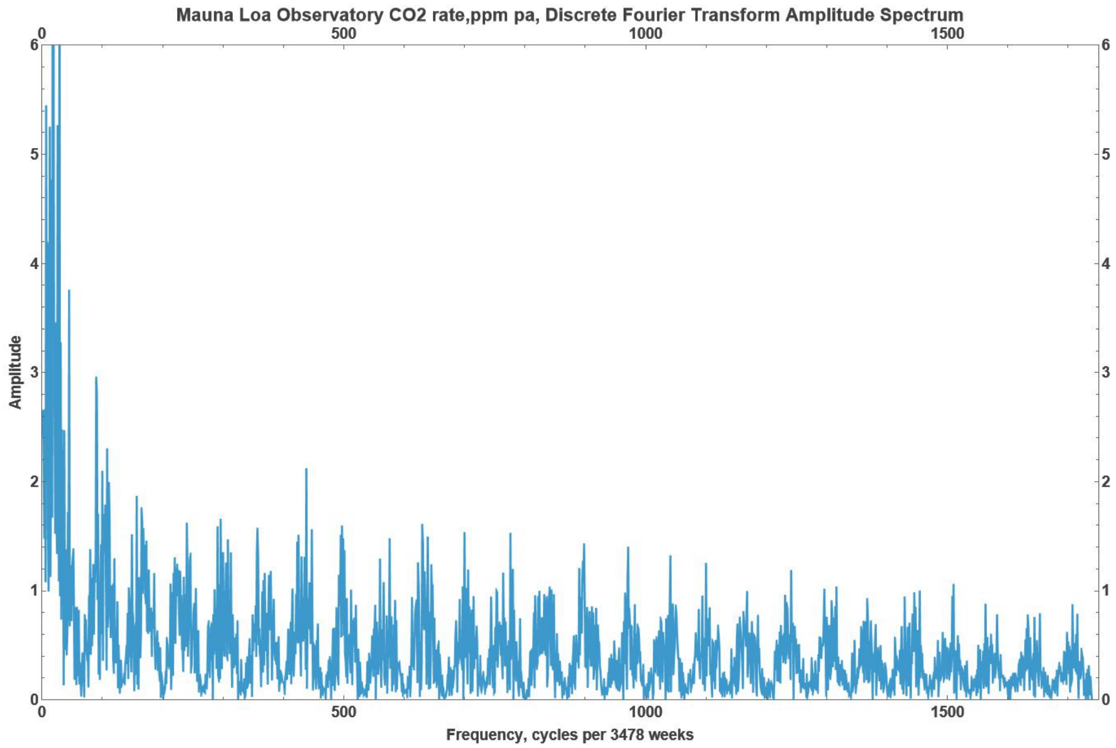

Figure 5. DFT Amplitude spectrum of the annual rate of change of CO_2 concentration.

There is a multitude of local maxima in the Amplitude spectrum some of which have been assigned possible sources from the known periods of the Moon and planets between instances of the Sun, Earth, Moon or planets being in alignment. Average values for these periods have been taken from the publicly available literature. The periods drift due to the ever changing configuration of the Solar System and this may contribute to a broadening of the spectral responses. There are other periodic events, such as changes in the ellipticity of the orbits which have not been taken into account in this study.

A list of possible sources is shown in Table 2 for a selection of the peaks in the DFT amplitude spectrum. They are listed by the coordinate on the x axis, in cycles per 3478 weeks, and the amplitude of response with periods in years and days for ease of reference to orbital periods of the Moon and planets. Some of these may also relate to the periodicities resulting from the Short-term orbital forcing described in Cionco, R. G., and Soon,W. W.-H.[Ref. 3].

Table 2

x-coord	Amplitude	years	days	possible source
7	5.42	9.52	3478.0	30 x Mercury, 6 x Venus synodic
18	8.48	3.70	1353.0	El Nino
29	6.02	2.30	839.5	7 x Mercury
45	3.73	1.48	541.0	20 x Moon draconic
90	2.93	0.74	270.5	10 x Moon draconic
102	1.67	0.65	238.7	2 x Mercury synodic
157	1.84	0.42	155.1	5 x Moon synodic
240	1.59	0.28	101.4	4 x Moon draconic
296	1.63	0.23	82.3	3 x Moon draconic
357	1.54	0.19	68.2	
379	1.15	0.18	64.2	
438	2.09	0.15	55.6	2 x Moon draconic
497	1.57	0.13	49.0	
576	1.45	0.12	42.3	
630	1.58	0.11	38.6	
700	1.50	0.10	34.8	
764	1.13	0.09	31.9	
776	1.50	0.09	31.4	
841	1.01	0.08	29.0	Moon synodic
898	1.40	0.07	27.1	Moon draconic
971	1.37	0.07	25.1	daily temperature cycle
1041	1.29	0.06	23.4	daily temperature cycle
1051	1.29	0.06	23.2	daily temperature cycle
1100	1.22	0.06	22.1	daily temperature cycle
1168	0.97	0.06	20.8	daily temperature cycle
1241	1.16	0.05	19.6	daily temperature cycle
1316	1.01	0.05	18.5	daily temperature cycle
1367	0.90	0.05	17.8	daily temperature cycle
1454	0.97	0.05	16.7	daily temperature cycle
1510	1.03	0.04	16.1	daily temperature cycle
1563	0.85	0.04	15.6	daily temperature cycle
1582	0.75	0.04	15.4	daily temperature cycle
1653	0.76	0.04	14.7	daily temperature cycle
1707	0.84	0.04	14.3	daily temperature cycle

Conclusion:

The major influence on the rate of generation of atmospheric CO_2 in the Equatorial zone has been the El Niño event, that is, climate change causing a change in the rate of generation of CO_2, the complete opposite to the UN IPCC claim that CO_2 causes climate change. As far as is known, no physical process has been proposed whereby the CO_2 change could cause an El Niño event.

Furthermore it is notable that both the synodic and draconic periods of the Moon are apparent throughout the 67 year weekly series. An explanation for the synodic period is that each New Moon reduces the incoming Sun's radiation to the Earth and its atmosphere as it passes between the Sun and the Earth. Similar temperature minima must occur when Mercury and/or Venus pass between the Sun and the Earth.

The draconic period is due to the Moon's elliptical plane being at an angle of 5.14° to the Earth's elliptic relative to the Sun. As a result, when the Moon passes through one of the two nodal points, where the Moon's ellipse intersects the Earth's elliptic, it has the greatest influence in diminishing the irradiation of the Earth which, in turn, reduces the Earth's surface temperature thereby causing a response in the rate of generation of CO_2.

Except during a Solar eclipse when the drop in temperature is obvious, the passing of the Moon through its nodal points may only cause a minor drop in temperature. In spite of this, there is a measurable effect on the rate of change of CO_2 concentration apparent in the amplitude spectrum implying a significant sensitivity between temperature and CO_2 rate of change. This action appears to have been completely overlooked by the UN IPCC in their assessment of the forces generating the Earth's climate.

As a number of the spectral maxima approximately correspond with the synodic periods of the Moon and the planets, the results are interpreted as showing that the Sun's irradiance of the Earth is modulated by the movement of the Moon and planets. This must cause corresponding changes in the Earth's sea-surface and atmospheric temperatures which, in turn, cause changes in the CO_2 concentration even down to the 24 hour daily cycle. This is contrary to the never-proven claim by the UN IPCC that increased CO_2 concentration causes an increase in the Earth's atmospheric and surface temperature.

The UN IPCC First Assessment Report, 1990, consisted of this Overview, quote:

This Overview reflects the conclusions of the reports of (i) the three IPCC Working Groups on science, impacts, and response strategies, and (ii) the Policymaker Summaries of the IPCC Working Groups and the IPCC Special Committee on the Participation of Developing Countries.
1. Science
This section is structured similarly to the Policymaker Summary of Working Group I.

1.0.1 We are certain of the following:
•There is a natural greenhouse effect which already keeps the Earth warmer than it would otherwise be.
•Emissions resulting from human activities are substantially increasing the atmospheric concentrations of the greenhouse gases: carbon dioxide, methane, chloro-fluorocarbons (CFCs) and nitrous oxide. These increases will enhance the greenhouse effect, resulting on average in an additional warming of the Earth's surface. The main greenhouse gas, water vapour, will increase in response to global warming and further enhance it.
End quote.

By 2021, the Sixth Assessment Report, AR6, Summary for Policymakers, Working Group I, declared, under "A. The Current State of the Climate"
A.1 It is unequivocal that human influence has warmed the atmosphere, ocean and land. Widespread and rapid changes in the atmosphere, ocean, cryosphere and biosphere have occurred.
End quote.

No such human influence has been detected by this analysis of the El Niño event, a major Earth climate event in spite of the 2015 Paris Agreement by 194 States and the European Union to tackle climate change nor the 2022 establishment of a UN High-Level Expert Group on Net-Zero Emissions Commitments of Non-State Entities. The fact is that the warming since the Little Ice Age has caused an ever changing increase in the temperature gradient between the Equator and the Poles which has resulted in changes in climate all across the Globe. Change requires action and action requires energy. CO2 is a simple molecule that does not produce energy so it cannot cause Climate Change.

In all likelihood, the UN together with the World Economic Forum are working to raise fear of climate catastrophe in the population at large so as to bring about the UN 'Pact for the Future' of One World Government on the assumption that the World will avoid a catastrophe once they control the World. As Klaus Schwab, Founder and Chairman, stated recently at the World Economic Forum 2025 in Davos: "The future doesn't just unfold, the future is shaped by us and especially by us in this room... "

References:

1. https://scrippsco2.ucsd.edu/data/atmospheric_co2/mlo.html
File: weekly_in_situ_co2_mlo.csv for the period 29 March 1958 to 29 November 2025.

2. Oceanic Nino Index, National Oceanic and Atmospheric Administration.
https://www.cpc.ncep.noaa.gov/products/analysis_monitoring/ensostuff/detrend.nino34.ascii.txt

3. Cionco and Soon, Short-term orbital forcing: A quasi-review and a reappraisal of realistic boundary conditions for climate modeling, Earth-Science Reviews 166 (2017) 206-222, Elsevier B.V.

Calculations performed using Wolfram Mathematica ver. 14.3.